Equilibrium Model of Bimodal Distributions of Epitaxial Island Growth

Robert E. Rudd*
Lawrence Livermore National Laboratory, Condensed Matter Physics Division, L-045, Livermore, California 94551

G. A. D. Briggs and A. P. Sutton
Department of Materials, University of Oxford, Parks Road, Oxford OX1 3PH, United Kingdom

G. Medeiros-Ribeiro
Laboratório Nacional de Luz Síncrotron, P.O. Box 6192, Campinas, SP 13084-971, Brazil

R. Stanley Williams
Hewlett-Packard Laboratories, 1501 Page Mill Road, Palo Alto, California 94304
(Received 29 May 2002; published 8 April 2003)

We present a nanostructure diagram for use in designing heteroepitaxial systems of quantum dots. The nanostructure diagram is computed using a new equilibrium statistical physics model and predicts the island size and shape distributions for a range of combinations of growth temperature and amount of deposited material. The model is applied to Ge on Si(001), the archetype for bimodal island growth, and the results compare well with data from atomic force microscopy of Ge/Si islands grown by chemical vapor deposition.

DOI: 10.1103/PhysRevLett.90.146101 PACS numbers: 68.35.Md, 68.35.Bs, 68.55.Jk, 68.65.–k

The usefulness of surface nanostructures for quantum dots and other applications depends on how well their size distributions can be understood and controlled. Self-assembled nanostructures can be grown epitaxially, with the crystal lattice of the island force-fitted to the crystal lattice of the substrate. The spontaneous formation of nanoislands relieves some of the resulting strain energy. There is a huge amount of data on the resulting distributions for many semiconductor systems. InAs/GaAs(001) exhibits well-defined distributions [1,2]; InP/GaInP shows characteristic bimodal size distributions, with at least two types of island [3]; the InGaN/GaN family remains to be charted. Here we present a statistical physics model that can account for the equilibrium distribution of sizes and shapes of any epitaxial system of self-assembled islands. The output is presented as a nanostructure diagram, which can do for surface nanomaterials what the phase diagram does for alloys: provide the tool to enable nanotechnologists to manipulate thermodynamics and kinetics as generations of metallurgists have done for the design of steels and other alloys. We have calculated a nanostructure diagram for Ge/Si(001) [4].

Many semiconductor nanostructures grow in a Stranski-Kranstanov mode. The first atoms deposit on the surface in epitaxial positions, and a flat wetting layer forms. In systems that form self-assembled nanostructures the wetting layer is generally in compression, matching the substrate lattice at the interface. The associated elastic strain energy increases with the thickness of the wetting layer, though this may to some extent be mitigated by surface defects [5]. If the mismatch strain is small, then eventually the strain may be relieved by interfacial dislocations. For larger mismatch strains the growth becomes three dimensional. The upper parts of the islands are free to relax, and the elastic energy released more than compensates for the increased surface energy. The shape and size distributions of the nanostructures depend on the temperature, T, and the amount of material deposited, to which we refer as equivalent coverage, θ. A model system is the growth of germanium on silicon, Ge/Si(001), and several experimental studies have been summarized in the form of a map with coverage and temperature as the two axes [6,7]. Note that this information is inherently different from that of a phase diagram in misfit strain vs coverage at zero temperature [8]. There has been controversy about the theory, much of which boils down to an argument about whether the process is thermodynamically or kinetically constrained [9]. Our surface nanostructure diagram enables the equilibrium size and shape distributions to be calculated and plotted as a function of coverage and temperature.

The core of the model is the statistical physics of the islands, which is governed by their energy and entropy. The internal energy has contributions from the internal energy of each island and the elastic interaction between pairs of islands,

$$\varepsilon_{\text{elastic}} = \sum_i \varepsilon_i^{(1)} + \sum_{i<j} \varepsilon_{i,j}^{(2)}. \tag{1}$$

The internal energy of the ith individual island of type I containing ν_i atoms is taken to be of the form [10]

$$\varepsilon_i^{(1)} = A^I \nu_i + B^I \nu_i^{2/3} + C^I \nu_i^{1/3} + D^I. \tag{2}$$

This form accounts for bulk effects due to elastic strain

relaxation (varying as ν), surface effects including reconstruction (varying as $\nu^{2/3}$), and edge effects such as interface strain concentration [varying as $\nu^{1/3}$, with a weak $\log(\nu)$ dependence suppressed] [11] and includes a size-independent term. The elastic interaction between pairs of islands [12] is treated in a self-consistent mean-field approach,

$$\bar{\varepsilon}_i^{(2)} = \frac{1}{2}\sum_{j\neq i}\varepsilon_{i,j}^{(2)} = \lambda\xi^2\nu_i^{2/3}\theta. \tag{3}$$

The interaction is of a dipole-dipole type, varying as the footprint of the island ($\sim\nu_i^{2/3}$) and the coverage θ [volume per unit area, or equivalent monolayers (ML)]. The leading parameters are λ which incorporates the elastic constants together with radial and angular distribution functions, and the square of the mismatch strain ξ. We spare the reader the full mathematical derivation of the calculation of the surface nanostructure diagram, but the heart of the calculation is to assume a chemical potential at a given surface coverage and temperature and calculate a grand partition function for the system assuming that the contribution of any one size of island is a negligibly small fraction of the total internal energy:

$$-\Omega/kT = \log\sum_{\text{configurations}} e^{-(E_{\text{total}}-N\mu)/kT} \tag{4}$$

$$= \log\prod_{\nu,I}\sum_{n_\nu^I}[e^{-n_\nu^I(E_\nu^i-\nu\mu)/kT}]/n_\nu^I! \tag{5}$$

$$\approx \sum_{\nu,I} e^{-(E_\nu^i[\theta(\mu)]-\nu\mu)/kT}, \tag{6}$$

where Ω is the grand potential, k is the Boltzmann constant, T is the absolute temperature, E_{total} is the total internal energy, E_ν^I is the mean-field single-island energy, N is the total number of atoms in all islands, μ is the chemical potential, and n_ν^I is the number of islands of type I containing ν atoms. Using Eq. (6), both the distribution and its fluctuations may be readily computed:

$$\langle n_\nu^I\rangle = e^{-(E_\nu^i[\theta(\mu)]-\nu\mu)/kT}, \tag{7}$$

$$\sigma_{\nu,I}^2 = \langle(n_\nu^I)^2\rangle - \langle n_\nu^I\rangle^2 = \langle n_\nu^I\rangle. \tag{8}$$

The corresponding coverage can be found from

$$\theta \approx \sum_{\nu,I}\nu\langle n_\nu^I\rangle. \tag{9}$$

Equation (8) indicates that the number of islands of a given type and size is a fluctuating quantity; $\sigma_{\nu,I}$ is a measure of the scatter in this number obtained by repeated experimental measurements.

The calculation is iterated by varying the chemical potential until self-consistency is achieved between the coverage calculated from the distribution and the coverage assumed in the mean-field expression for the island-island interaction. In particular, the sum over ν in Eq. (9), approximated by an integral, has been computed analytically with a saddle point technique that converges rapidly even for integration over rather broad, asymmetric functions like the island distributions (shown below) [13]. The resulting nonlinear equation is solved numerically for $\mu(\theta, T)$. Once the chemical potential is known, the island distributions specified by Eq. (7) provide the data for calculating the nanostructure diagram.

The nanostructure diagram for Ge/Si(001) is presented in Fig. 1. A surface with 8 ML Ge grown at 600 °C exhibiting pyramids and domes is shown in the inset. The horizontal axis is coverage θ and the vertical axis is temperature T. The color scale in the diagram indicates the relative numbers of pyramids and domes at each combination of coverage and temperature. The island internal energy parameters were deduced by fitting these calculated distributions to experimental data. In order to have a minimum in the cubic energy expression [2], B and C in Eq. (2) must have opposite signs. Since a Ge(001) surface does not spontaneously roughen, B is expected to be positive, and our fitting follows this (with $A-\mu<0$, $C<0$). However, since 3D island growth is preceded by multiplication of defects in the Ge wetting layer [7], with their own associated energy, B could be negative (with $A-\mu>0$, $C>0$) [4]. With $B>0$, the increase in

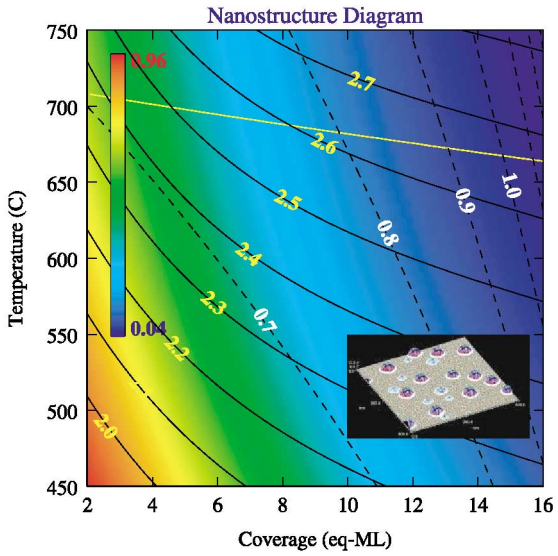

FIG. 1 (color). The nanostructure diagram for Ge/Si(001). The inset scanning tunneling micrograph shows pyramids and domes of different sizes coexisting in equilibrium next to each other, grown by Ge molecular beam epitaxy on Si(001) at 3 ML/min at 600 °C to give a coverage $\theta = 8$ ML. The rainbow color scale indicates the relative numbers of pyramids (4%–96%). The solid yellow line is a contour of relative dome population at the maximum in the island energy and gives an indication of the onset of unstable ripening. The contours indicate relative distribution widths [normalized to the mean island size: pyramids (solid lines); domes (dashed lines)], illustrating the wealth of information that is contained in the nanostructure diagram.

surface energy is more than compensated by a decrease in bulk and edge elastic energies. Of the three terms, C has been discussed least in the literature. It contains the physics of the surface stress and the elastic relaxation around the edges [10]. Another effect is the trenching seen around many islands [5]. If this effect is energetically driven, then it too would give a contribution that scales like $\nu^{1/3}$ and reduce the energy, as would the rounding of edges of an island. To perform the fitting we had to ensure that the distribution was negligible at the maximum in the cubic and constrain it to vanish beyond it. Although we have up to four parameters for each nanostructure type, plus one for the mean-field interaction, the model is based on sound theory and the parameters are obtained by fitting to over 100 data points summarizing measurements on tens of thousands of nanostructures. Table I contains the fitted parameters. In general, the terms in Eq. (2) correspond to a small fraction of the overall energy, so nanostructure systems with bimodal equilibrium distributions exhibit fine tuning.

Since the nanostructure diagram is so rich in content it presents a challenge in information presentation, which can ultimately be met only by an interactive multimedia display. In Fig. 1 we have plotted contours of constant width of the relative size distribution for pyramids and domes. Figure 2 illustrates the distribution curves calculated at each point, together with experimental data of the kind used to determine the parameters in Table I. In some ways the nanostructure diagram is like a phase diagram; for example, at 600 °C the volume of Ge in pyramids and in domes obeys something like a lever rule between about 3 and 5 eq ML [4]. But this is only approximately true, partly because we are dealing with thermodynamics of small systems [14] and also because the analogy between phases and nanostructure types is limited. There are no absolute boundaries in the nanostructure diagram; the populations decay exponentially where they are not favored. The time-consuming part of the calculation is finding the chemical potential; we have formulated an empirical expression for the chemical potential to enable a fast point-and-click presentation and analysis of the distributions to be implemented.

TABLE I. Parameters for the single-island (2) and mean field (3) contributions to the island energy (1) as a function of island type and size. For comparison, the elastic strain energy in unrelaxed epitaxial Ge/Si would be 0.038 eV/atom, and the total surface energy would be about 50 eV for a pyramid of volume 1000 nm^3. The parameter A is relative to an arbitrary zero which is subject to variation depending on the chemical potential; regardless of the number of digits given none of the parameters is reliable to more than two significant figures. The parameters were deduced from χ^2 fitting to data from tens of thousands of islands grown at 600 °C with coverages $\theta = 2.2$, 4.7, 7.2, 9.0, and 11.8 ML. The units are eV/atom^m, where $m = 1, \frac{2}{3}, \frac{1}{3}, 0$ for A, B, C, D, respectively, and eV/atom$^{2/3}$/ML for $\lambda\xi^2$

Parameter	Pyramids	Domes
A	-9.60×10^{-6}	-5.137×10^{-6}
B	9.0286×10^{-4}	1.0834×10^{-3}
C	-0.04517	-0.1396
D	0.1422	4.1625
$\lambda\xi^2$	2.305×10^{-5}	1.974×10^{-5}

The nanostructure diagram shows a crossover from almost complete dominance of pyramids at low coverage and low temperature to dominance of domes at high coverage and high temperature. The trend from pyramids to domes with increasing coverage at constant temperature results from island-island repulsion; the trend from pyramids to domes with increasing temperature at constant coverage results from an endothermic transition. The island-island repulsion is also responsible for the increase in the relative width of both dome and pyramid transitions with coverage (through a flattening of the minima in the energy curves); the increase with temperature is due to thermal fluctuations. The model assumes equilibrium, but it contains an indication of where unrestrained ripening would occur: at high temperatures [above 700 °C for Ge/Si(001)] the minimum in the distribution for large domes can no longer be approximated as zero, and large domes that formed would be unstable to continued ripening. This model treats the diffusion of Ge atoms between the islands and the wetting layer as a dynamic equilibrium. The constraint that the number of Ge atoms is constant is translated into a chemical potential associated with the wetting layer. This is a significant advance. There have been no previous calculations of the chemical potential in equilibrium island growth, and it is what makes our model work. The chemical potential is computed explicitly and self-consistently with regard to the island-island interaction and lies at the heart of our determination of the island distributions.

How valid is the assumption of equilibrium? At best it is only an approximation, because at the true equilibrium the germanium is simply dissolved in the bulk silicon, and no surface nanostructure survives. Kinetic effects have been noted in many island growth experiments. Dynamic coarsening of Ge/Si(001) nanostructures has been directly observed [15] and accounted for in terms of an anomalous coarsening model. The bimodal size distribution of InP/GaInP nanostructures depends on the growth rate [16]. Nucleation rate dependence can be tested by a scaling law [17] provided there is not a change of mechanism during growth, but even InAs/GaAs(001), which generally gives a monomodal distribution, can also exhibit a bimodal distribution [18]. However, following long anneals of Ge/Si(001) at 550 °C the island distribution ceased to evolve and islands of markedly different sizes were found to coexist next to each other [19]. This observation provides evidence for equilibrium rather than unstable ripening.

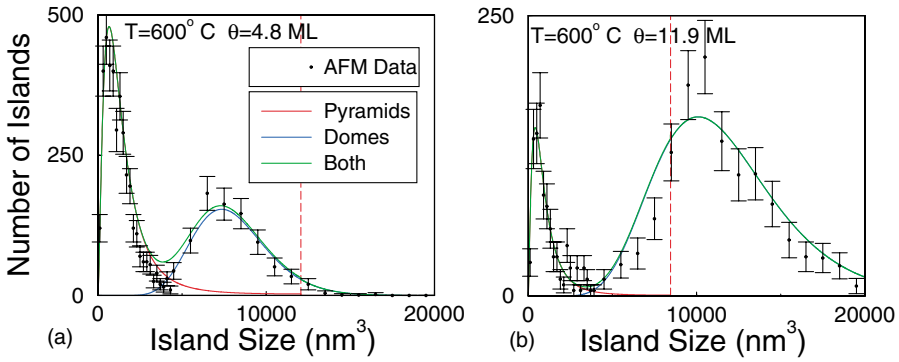

FIG. 2 (color). Island size distributions illustrating the information that is available at each point on the nanostructure diagram. The curves give the numbers of islands of each type from Eq. (7), and the total number at $T = 600\,^{\circ}\mathrm{C}$ and (a) $\theta = 4.8$ ML Ge/Si(001); (b) $\theta = 11.9$ ML Ge/Si(001). The vertical scales are different. The bimodal size distribution is characteristic of two island types. Experimental data are also plotted. The broken vertical line indicates the turning point in the pyramid energy at which the distribution was truncated; in both cases the equivalent point for domes is beyond 100 000 nm^3.

The goal of the nanostructure diagram is to provide a tool to use the kinetic effects and the underlying equilibrium state to attain a desired island distribution. To this end, different kinetic effects can be incorporated in the equilibrium model. Insofar as alloying is uniformly distributed [20,21] it can be accounted for by appropriate constants in Eqs. (2) and (3); generally the mean equilibrium nanostructure volume varies inversely as the sixth power of the mismatch [19]. Alloying constrains the temperature range over which experiments can be performed. At 600 °C Ge/Si islands can fairly rapidly achieve equilibrium between themselves before significant alloying occurs; at 550 °C the approach to nanostructure equilibrium is already rather slow [22], and at 650 °C alloying already occurs rapidly. One kinetic barrier present in the existing model is the barrier to nucleate an island sufficiently large for unlimited ripening. The minimum in the island distribution (cf. Fig. 2) offers an indication of the balance between thermodynamics and kinetics distinct from a moment analysis [13,23].

The model could be extended to account for modest kinetic effects by allowing the chemical potentials of the different nanostructure types to be different from each other and from the wetting layer. A rate equation could then be set up to describe the approach to equilibrium. In this way we may be able to achieve convergence between our model and kinetic Monte Carlo calculations and hence make further progress toward a complete thermodynamic and kinetic toolbox for nanotechnologists.

This work was performed in part under the auspices of the U.S. Department of Energy by the University of California, Lawrence Livermore National Laboratory, under Contract No. W-7405-Eng-48.

*Electronic address: robert.rudd@llnl.gov

[1] R. Leon *et al.*, Phys. Rev. Lett. **81**, 2486 (1998).
[2] B. A. Joyce *et al.*, Mater. Sci. Eng. B **67**, 7 (1999).
[3] C. M. Reaves *et al.*, Surf. Sci. **326**, 209 (1995); C. M. Reaves*et al.*Surf. Sci.cf. **341**, 29 (1995).
[4] R. S. Williams, G. Medeiros-Ribeiro, T. I. Kamins, and D. A. A. Ohlberg, Annu. Rev. Phys. Chem. **51**, 527 (2000).
[5] I. Goldfarb, P. T. Hayden, J. H. G. Owen, and G. A. D. Briggs, Phys. Rev. Lett. **78**, 3959 (1997).
[6] M. Tomitori, K. Watanabe, M. Kobayashi, and O. Nishikawa, Appl. Surf. Sci. **76**, 322 (1994).
[7] I. Goldfarb *et al.*, Surf. Sci. **394**, 105 (1997).
[8] I. Daruka and A.-L. Barabasi, Appl. Phys. Lett. **72**, 2102 (1998).
[9] M. Meixner, E. Schöll, V. A. Shchukin, and D. Bimberg, Phys. Rev. Lett. **87**, 236101 (2001).
[10] V. A. Shchukin, N. N. Ledentsov, P. S. Kop'ev, and D. Bimberg, Phys. Rev. Lett. **75**, 2968 (1995); V. A. Shchukin and D. Bimberg, Rev. Mod. Phys. **71**, 1125 (1995).
[11] G. Medeiros-Ribeiro *et al.*, Science **279**, 353 (1998).
[12] J. A. Floro *et al.*, Phys. Rev. Lett. **80**, 4717 (1998).
[13] R. E. Rudd *et al.* (to be published).
[14] T. L. Hill, *Thermodynamics of Small Systems* (Dover, New York, 1994).
[15] F. M. Ross, J. Tersoff, and R. M. Tromp, Phys. Rev. Lett. **80**, 984 (1998).
[16] J. Porsche, A. Ruf, M. Geiger, and F. Scholz, J. Cryst. Growth **195**, 591 (1998).
[17] J. G. Amar and F. Family, Phys. Rev. Lett. **74**, 2066 (1995).
[18] H. Saito, K. Nishi, and S. Sugou, Appl. Phys. Lett. **74**, 1224 (1999).
[19] W. Dorsch *et al.*, Appl. Phys. Lett. **72**, 179 (1998).
[20] X. Z. Liao *et al.*, Phys. Rev. B **60**, 15 605 (1999).
[21] X. Z. Liao *et al.*, Appl. Phys. Lett. **77**, 1304 (2000).
[22] G. Medeiros-Ribeiro, T. I. Kamins, D. A. A. Ohlberg, and R. S. Williams, Phys. Rev. B **58**, 3533 (1998).
[23] T. I. Kamins, G. Medeiros-Ribeiro, D. A. A. Ohlberg, and R. S. Williams, J. Appl. Phys. **85**, 1159 (1999).